

NOTA DI LAVORO

76.2014

Delineating Spring Recharge Areas in a Fractured Sandstone Aquifer (Luxembourg) Based on Pesticide Mass Balance

By J. Farlin, CRP Henri Tudor (Luxembourg)
L. Drouet, Fondazione Eni Enrico Mattei
T. Gallé, CRP Henri Tudor (Luxembourg)
D. Pittois, CRP Henri Tudor (Luxembourg)
M. Bayerle, CRP Henri Tudor (Luxembourg)
C. Braun, CRP Henri Tudor (Luxembourg)
P. Maloszewski, Helmholtz Zentrum,
Munich (Germany)
J. Vanderborght, Helmholtz Zentrum,
Jülich (Germany)
M. Elsner, Helmholtz Zentrum,
Munich (Germany)
A. Kies, University of Luxembourg

Climate Change and Sustainable Development

Series Editor: Carlo Carraro

Delineating Spring Recharge Areas in a Fractured Sandstone Aquifer (Luxembourg) Based on Pesticide Mass Balance

By J. Farlin, CRP Henri Tudor (Luxembourg)
L. Drouet, Fondazione Eni Enrico Mattei
T. Gallé, CRP Henri Tudor (Luxembourg)
D. Pittois, CRP Henri Tudor (Luxembourg)
M. Bayerle, CRP Henri Tudor (Luxembourg)
C. Braun, CRP Henri Tudor (Luxembourg)
P. Maloszewski, Helmholtz Zentrum, Munich (Germany)
J. Vanderborght, Helmholtz Zentrum, Jülich (Germany)
M. Elsner, Helmholtz Zentrum, Munich (Germany)
A. Kies, University of Luxembourg

Summary

A simple method to delineate the recharge areas of a series of springs draining a fractured aquifer is presented. Instead of solving the flow and transport equations, the delineation is reformulated as a mass balance problem assigning arable land in proportion to the pesticide mass discharged annually in a spring at minimum total transport cost. The approach was applied to the Luxembourg Sandstone, a fractured-rock aquifer supplying half of the drinking water for Luxembourg, using the herbicide atrazine. Predictions of the recharge areas were most robust in situations of strong competition by neighbouring springs while the catchment boundaries for isolated springs were extremely sensitive to the parameter controlling flow direction. Validation using a different pesticide showed the best agreement with the simplest model used, whereas using historical crop-rotation data and spatially distributed soil-leaching data did not improve predictions. The whole approach presents the advantage of integrating objectively information on land use and pesticide concentration in spring water into the delineation of groundwater recharge zones in a fractured-rock aquifer.

This is a pre-print version of the article "Delineating spring recharge areas in a fractured sandstone aquifer (Luxembourg) based on pesticide mass balance" published in Hydrogeology Journal June 2013, Volume 21, Issue 4, pp 799-812, DOI 10.1007/s10040-013-0964-5

Keywords: Spring Protection Zones, Atrazine, Luxembourg, Fractured Rock, Groundwater Pollution

JEL Classification: Q5, Q53

Address for correspondence:

Julien Farlin
CRP Henri Tudor, CRTE Technoport Schlassgoart
66, rue de Luxembourg
L-4002 Esch-sur-Alzette
Luxembourg
Phone : +352 425991 4648
E-mail: julien.farlin@tudor.lu

Delineating spring recharge areas in a fractured sandstone aquifer (Luxembourg) based on pesticide mass balance

J. Farlin¹, L. Drouet², T. Gallé³, D. Pittois³, M. Bayerle³, C. Braun³, P. Maloszewski⁴, J. Vanderborght⁵, M. Elsner⁴, A. Kies⁶

Abstract

A simple method to delineate the recharge areas of a series of springs draining a fractured aquifer is presented. Instead of solving the flow and transport equations, the delineation is reformulated as a mass balance problem assigning arable land in proportion to the pesticide mass discharged annually in a spring at minimum total transport cost. The approach was applied to the Luxembourg Sandstone, a fractured-rock aquifer supplying half of the drinking water for Luxembourg, using the herbicide atrazine. Predictions of the recharge areas were most robust in situations of strong competition by neighbouring springs while the catchment boundaries for isolated springs were extremely sensitive to the parameter controlling flow direction. Validation using a different pesticide showed the best agreement with the simplest model used, whereas using historical crop-rotation data and spatially distributed soil-leaching data did not improve predictions. The whole approach presents the advantage of integrating objectively information on land use and pesticide concentration in spring water into the delineation of groundwater recharge zones in a fractured-rock aquifer.

¹ Corresponding author. Address : CRP Henri Tudor, CRTE, Technoport Schlassgoart, 66, rue de Luxembourg, L-4002 Esch-sur-Alzette, Luxembourg. Tel : +352 425991 4648. Email address : julien.farlin@tudor.lu

² Fondazione Eni Enrico Mattei, Milan, Italy

³ CRP Henri Tudor, CRTE, Luxembourg

⁴ Helmholtz Zentrum, Institute for Groundwater Ecology, Munich, Germany

⁵ Helmholtz Zentrum, Institute of Bio-and Geosciences, Jülich, Germany

⁶ University of Luxembourg, Physics Department, Luxembourg

Keywords: spring protection zones, atrazine, Luxembourg, fractured rock, groundwater pollution

1. Introduction

The large number of scientific publications and guidelines pertaining to the modeling of flow and transport in fractured rock aquifers in general and to the delineation of protection zones in particular is a telling testimony of both the difficulty and relevance of the task (for a review, see Bodin et al., (2003), and for example applications, Stauffer et al., (2002) and USEPA, (1991)). Although numerical groundwater models can be implemented in a fractured-rock setting, the large number of fitting parameters precludes practical applications in all but a few exceptionally well-documented cases (Cacas et al., 1990). In most practical situations, the hydrogeological investigations necessary to estimate the hydraulic parameters of the aquifer would be extremely costly to be applied regionally. Because of this, engineering offices often rely, for heterogeneous aquifers, on surface-morphology oriented approaches (isochrone methods, DISCO (Pochon and Zwahlen, 2003)) that include surface mapping of vulnerable areas and the use of tracers to detect preferential pathways. The information gained is usually analysed with a geographic information system (GIS), organized into layers and aggregated using subjective weighting based on experience and expert knowledge. A widely recognized technique to assess flow paths, travel time, and the vulnerability of an aquifer consists of injecting artificial tracers and monitoring their breakthrough in the aquifer's outlets (Käss, 1998, Maloszewski et al., 1998). Artificial tracers have two major limitations: they yield only point information on the system in both space and time, and their use is restricted to aquifers with transit times of a few months at most, as the sampling time would otherwise increase beyond the logistically and economically feasible. At the catchment scale, artificial tracers can be replaced by so called environmental tracers, which have the advantage of entering the aquifer naturally during recharge either as part of the water molecule (tritium, deuterium, oxygen 18) or as a gas or solute (chlorofluorocarbons, carbon 14). Fractured aquifer systems have indeed been successfully characterized hydrogeologically using a

combination of environmental tracers (Maloszewski et al., 2002, Zuber and Motyka, 1994). Water isotopes were used in the present study to estimate the mean groundwater residence time and the contribution of fast flow to spring discharge. However, because such tracers are applied approximately homogeneously at the scale of the catchment, they do not carry any discriminating piece of information about different spatial attributes which may be of interest within it. This gap can be filled by point-source or diffuse pollutants. Pathogens have been used for instance in karst hydrology as indicators to pinpoint pollution sources and estimate groundwater storage (Ryan and Meiman, 1996). Although nutrients and pesticides could serve the same purpose, there has been, to the authors' knowledge, no attempt until now to integrate this information into a quantitative analysis. In this paper, an approach to compute the recharge area of a spring respecting the pesticide mass balance is presented. By leaving aside the flow and transport equations, the need to explicitly model the complex fracture network of the sandstone was circumvented. The cornerstones of the study were as follows: 1) Estimation of the pesticide transport time in the soil and in the aquifer using a combination of tritium measurements and numerical modeling techniques 2) Evaluation of the stability of the pesticide signal in spring water with the help of stable isotopes and monitoring of pesticide concentration in spring water 3) Delineation of the springs' recharge zones from the pesticide mass balance.

2. Material and method

2.1 Study area

Although an important drinking water supply and impacted by pollutants at the regional scale, the springs and wells of the Luxembourg Sandstone still lack protection zones and a scientifically sound and cost-effective method to delineate them. The aquifer of the Luxembourg Sandstone, which provides about half of the country's drinking water, is a prominent geological and geomorphological feature of southern Luxembourg, a region known as Gutland, where it forms a striking landscape of cuestas and cliffs. Due to a gentle dip towards the southwest (less than 10°), the Luxembourg Sandstone of the Early Jurassic, still

unconfined in its northern part, progressively plunges below the marls of Strassen, where it becomes confined (Colbach, 2005). The Sandstone itself, up to 100 meters thick, is underlain by the marls of Elvange acting together with the Rhaetian Clays (Late Triassic) as aquiclude.

Porosity follows a bimodal distribution, with a primary porosity reported to be between 5% and 40%, depending on the degree of dissolution of the calcareous matrix and a secondary fracture porosity estimated to 1% (Colbach, 2005). Folds and faults resulting from tectonic deformations are both significant controls of groundwater flow. Fractures strike along two main directions: North-West and North-East. In its unconfined part, the sandstone is drained by numerous contact springs whose occurrence and spatial distribution partially reflect the alternation of synclines and anticlines and the location of major fault blocks striking mainly SW-NE (Lucius, 1943). The physical and geochemical properties of the formation are heterogeneous, dense hard sandstone layers alternating with brittle limestone.

The effect of fracturing on groundwater flow and pollutant transport at the catchment scale has been the subject of much conjecture (Benbrahim, 2004, Gourdol et al., 2010), but little sound scientific evidence is available concerning the influence of the fracture network at the catchment scale and its regional variability. Because the sandstone is mainly covered by well-drained sandy soils, the potential for groundwater contamination by agricultural activities is high, and pollution by herbicides or nitrate widespread. Rapid breakthrough of artificial tracers has been reported by engineering offices, and excavations in the vicinity of spring catchworks draining the sandstone have sometimes revealed large water-bearing fractures, suggesting the aquifer transmits water in ways comparable to a karstic formation. The contribution of rapid fracture-flow might however be only significant in a few reactive springs and negligible in the majority of cases.

The delineation tool was developed for the Steinsel plateau, which is located ten kilometers north-west of Luxembourg City. The sandstone formation sits like a slab on its subhorizontal marly aquiclude, approximately hundred meters above the valleys and measuring seven

kilometer from north to south and one kilometer from east to west, the overburden of the marls of Strassen being completely absent (figures 1 & 2). The aquifer has an average thickness of 55 meters (maximum 80 meters), with a saturated zone of 10 meters or less and a thick unsaturated zone of up to 70 meters. The thickness of the underlying marls of Elvange is 20 meters at the vertical of the observations well. The centre of the plateau is occupied by arable land surrounded by woods also covering the slopes. The plateau is bounded on its western side by the Mamer Valley and on its eastern side by the Alzette Valley. The agricultural areas, situated in the center of the plateau, are divided by woodland into a northern and a southern region (opposite K1-K7 in figure 1). The soils are mainly sandy loams with some loamy sand lenses present, the largest of these being in the southern region. Besides crop land, three commercial orchards can be found in the study area. Soil depth varies between 1 and 2 meters. The aquifer is drained by numerous springs, mostly emerging close to one another on the western side. The majority are tapped and used as drinking water supply by the city of Luxembourg. On the Alzette River side, fewer springs can be found and most of them are used by the neighbouring towns. Discharge varies from spring to spring from a few liters per minute to more than 300 l/min. The slight dip of the Sandstone's base to the South-West probably exerts some control on groundwater flow and probably explains the unequal distribution of springs between western and eastern slopes. Groups of springs, common on the western slope, probably mark the presence of local synclines. A mean annual groundwater recharge of 180 ± 25 mm was estimated from spring discharge (for an uncertainty in discharge measurement of 15%). Since neither diffuse discharge nor the precise southern extent of the recharge area is known, this value is probably an underestimate.

Nearly all the springs in the area are contaminated to some degree by at least one phytosanitary compound. Some tapped springs had to be abandoned because of pesticides exceeding the legal threshold or recurrent bacterial proliferation.

2.2 Model assumptions

A combination of isotopic data, mass balance calculation and numerical modeling techniques were used to verify whether the aquifer, despite its fractured nature, can be treated as a homogeneous block at the catchment scale. For the purpose of delineating the recharge zones, the system composed by the soil and aquifer compartments is treated as time-invariant. Hence, the time-dependent variables, discharge and pesticide concentration in spring water and in recharge water, are averaged to mean values. While the assumption may hold well for groundwater systems dominated by the slow flow component with mean residence times (water and solute) of at least a few years, the approach is not applicable to springs that display strong seasonal or event-driven variations in discharge and pesticide load (karstic springs for example). Consequently, the model makes the following assumptions concerning the transmission and modification of the pesticide signal through the soil and aquifer systems:

- Pollutant concentration in the springs is in good approximation at steady-state over a time scale of several years, without significant fast flow bursts and seasonal or pluriannual variations.
- The soil's and the aquifer's dispersivities are high enough to smooth the unsteady pesticide flux in the soil due to intermittent application of pesticides and variable meteorological boundary conditions, i.e. the combined residence time in the soil and aquifer compartment is much longer than the time scale of pesticide flux variations.
- Fast transport components short-circuiting the aquifer are negligible compared to the slow flow.
- After leaving the soil/weathered zone, pesticides behave conservatively, i.e. sorption and degradation in the aquifer are negligible.

The validity of these assumptions will each be discussed in turn.

2.3 Sampling and analysis

All springs shown in figure 1 were sampled on a monthly basis for two years (March 2008 to March 2010), and seven springs weekly over a year and a half. Additionally, a monitoring well was drilled at the outskirts of the forest on the western side of the plateau and sampled weekly as well from March 2009 to March 2010. Sampling included water chemistry and pesticide concentration, tritium and stable water isotopes, field discharge, temperature and electrical conductivity. Five of the springs sampled weekly were also equipped with online probes measuring discharge, temperature and electrical conductivity at ten minute intervals. Time domain reflectometry (TDR) probes measuring soil moisture content were installed on one field in four vertical profiles. Crop rotation data from 2006 to 2009 for the entire plateau were also available.

Pesticide concentrations of the water samples were determined using an LC-ESI-MS/MS (liquid chromatography-electrospray ionization-tandem mass spectrometry) system Finnigan TSQ Quantum Discovery MAX with a Finnigan Surveyor LC Pump Plus and a Finnigan Surveyor MS Pump Plus (Thermo Electron Corporation, San José, CA, USA). The samples were injected using an autosampler HTC-PAL (CTC Analytics AG, Zwingen, Switzerland). The separation of the target compounds was carried out with a column Hypersil Gold aQ, 100 x 2.1 mm with 3 µm particle size (Thermo Scientific, Geel, Belgium). The elution was started with 70/30 ultrapure water (18 MΩ) / Methanol (acidified with 0.1 % formic acid) with a flow rate of 0.2 ml per minute. During the acquisition, methanol was increased to 100 %. The water samples were analysed with a LC-MS coupled with online extraction. A pre-column acting as an extraction column was interconnected between the autosampler injection valve and the chromatography column (Hpersil Gold, 20 x 2.1 mm, particle size 12 µm from Thermo Scientific, Geel, Belgium). Per measurement cycle, 1 mL was injected into the system and extracted with the pre-column. Afterwards, the target compounds were separated at the chromatography column and analysed at the triple quadrupole mass spectrometer.

Stable isotopes of oxygen and hydrogen were determined using isotope mass spectrometry. The water samples for oxygen isotopic analyses were prepared by conventional H₂O–CO₂ equilibration (Epstein and Mayeda, 1953) where 5 ml of each sample were equilibrated with CO₂ gas at 25 ± 0.1°C for 24 h. The CO₂ gas was then extracted and cryogenically purified in a vacuum line. For hydrogen isotope analysis (D/H) water samples were reduced to molecular hydrogen in a uranium reactor, and the gas was subsequently introduced into the inlet of an isotope ratio mass spectrometer (Delta-S, Finnigan MAT, Germany). Calibration was accomplished with three in-house standards that were calibrated against the international reference materials VSMOW, SLAP and GISP (IAEA, Vienna).

Tritium measurements were conducted by liquid scintillation counting of water after electrolytic enrichment following Eichinger et al. (1980).

2.4 Soil dynamics

The atrazine transit time through the soil compartment was studied using the numerical code PEARL (Leistra et al., 2001). The model was chosen because of the completeness of its documentation and the implementation of standard scenarios (FOCUS, 2000) and crop parameter library that could serve as a template. PEARL is a one-dimensional code simulating transient water and pesticide transport in unsaturated media. In a first step, the water fluxes (infiltration, evaporation, plant uptake and transpiration) are calculated by the hydrological module SWAP (van Dam et al., 1997), and in a second step, pesticide transport and degradation is simulated by PEARL. Studies have shown that substance-specific parameters describing the fate of a pesticide in the soil compartment can be extremely variable in the field, and values presented as typical in registration reports can give misleading estimates of the effective in-situ mobility and resilience of pesticides (Allen and Walker, 1987, Dubus et al., 2003). Furthermore, soil parameters affecting pesticide transport and degradation can vary spatially within a range that also affects pesticide leaching (Eckhardt and Wagenet, 1996, Jura and Gruber, 1989) and even the simulation of water flow

cannot always be described precisely when measurements made using complex systems such as lysimeters are not available. Hence, considering the large uncertainties associated with predicting leaching values, the model PEARL was used solely to calculate the time delay between the initial pesticide application and the onset of leaching out of the soil column, as well as the time after which pesticide concentration in leaching water starts to decrease following the last application. Absolute leaching values adopted for the delineation itself were calculated from mass balance, as detailed further below.

PEARL was calibrated hydraulically using the TDR data and the annual recharge rate calculated from the water balance. Soil moisture measurements at different depths over six months were combined into three sets. For each set, van Genuchten parameters (except the saturated hydraulic conductivity) were first estimated inversely using the software PEST (Doherty, 2009). The saturated hydraulic conductivity parameter was then adjusted until the model predicted an annual groundwater recharge equal to the calculated value of 180 mm. Three different hydraulic models were eventually obtained. The agreement between observed and measured soil moisture was poor (r^2 ranging from 0.24 to 0.38) and could be due to uncertainties in the estimation of daily evapotranspiration, which was calculated using the Penman-Monteith formula (Allen et al, 1998). In the next step, the parameters describing atrazine sorption and degradation were estimated from atrazine concentrations measured in the monitoring well for each hydraulic model, again using PEST. For this step, long-term leaching (20 years) was simulated by using synthetic precipitation time series generated using a first-order Markov chain (Wilks and Wilby, 1999) calibrated with data from Pfister et al. (2005) and the Luxemburgish national weather service. This approach was preferred over using measured rainfall for two reasons: the dearth of accurate data for the time period before 2000, and the possibility offered by synthetic rainfall to generate different realizations useful for sensitivity analysis. Potential evapotranspiration was calculated from the Transys dataset (Marion and Urban, 1995) representing a typical year for the normal period 1960-1990 for the closest meteorological station situated in Trier, Germany. All meteorological

boundary conditions were repeated for each year of the simulations. Application frequency was varied from once every year to once every four years. Transient simulations of atrazine leaching were performed for the three calibrated models to predict the time lag between the first/last atrazine application and the onset/the end of its release from the soil column.

2.5 Groundwater dynamics

Spring discharge is the sum of a slow flow component with long residence times (months to years) and a fast flow component. The average pesticide concentration observed in the springs is representative for the aquifer system as a whole only if the discharge is nearly completely sustained by slow flow. The delineation tool also assumes the existence of a stable regime in the pesticide concentration measured in the spring over a few years. Such a stable regime can be expected for a well-buffered aquifer system characterized by long mean residence times that smooth out peaks in pesticide application. More details of the hydrogeological characterization and atrazine transport in the aquifer of the study area can be found in Farlin et al. (2013).

Stable isotopes were used to study the fast flow dynamics. At the outlets of groundwater systems with mean residence times greater than two or three years, the signal of stable isotopes ($\delta^{18}\text{O}$ and $\delta^2\text{H}$) in recharge water, which displays a distinct seasonal variation with a maximum during the summer months, has leveled off to the mean annual recharge value (Clark and Fritz, 1997). Deviations from that mean isotopic value indicate an increase of the fast flow component mixing with slow flow at the outlet.

While stable isotopes give insight into groundwater residence times of up to a few months, tritium allows dating waters with mean residence times up to a few decades (Clark and Fritz, 1997). Using lumped-parameter models, one can estimate the mean residence time of water in the aquifer. The relation between tritium input $C_{in}(t)$ and output $C_{out}(t)$ is given by a convolution integral using a travel time distribution function g

$$(1) \quad C_{\text{out}}(t) = \int_0^{\infty} C_{\text{in}}(t-\tau)g(\tau)\exp(-\lambda_{\text{tracer}}\tau)d\tau$$

Where t is time, λ_{tracer} is the degradation rate of the tracer [1/T] (12.3 years for tritium) and $g(t)$ is the travel time distribution [1/T].

An exponential piston-flow transfer function was selected to simulate the dual residence time distribution (approximately equal for all flow lines in the unsaturated zone and exponentially distributed in the saturated zone)

$$(2) \quad g(\tau) = \frac{\eta}{t_{\text{epm}}} \exp\left(-\frac{\eta\tau}{t_{\text{epm}}} + \eta - 1\right) \text{ for } \tau \geq t_{\text{epm}}(1 - \eta^{-1})$$

$$g(\tau) = 0 \text{ for } 0 < \tau < \frac{\eta - 1}{\eta} t_{\text{epm}}$$

with η =dimensionless ratio of entire volume of water in storage to volume of water in the saturated zone and t_{epm} =mean transit time [T]

Since the transfer function describes the transit time distribution resulting from the flowtime of separate streamlines contributing water to a spring, it can be used to predict pesticide evolution over time, assuming no sorption within the aquifer (Eq. 3). The transfer function g however has to be modified to account for the fact that atrazine is not applied uniformly over the catchment, but only on agricultural surfaces (Farlin et al., 2013).

$$(3) \quad C'_{\text{out}}(t) = n \int_{-\infty}^t C'_{\text{in}}(\tau)g'(t-\tau)\exp[-\lambda_{\text{pesticide}}(t-\tau)]d\tau$$

with $C'_{\text{in}}(\tau)$ and $C'_{\text{out}}(\tau)$ respectively the atrazine input and breakthrough [M/L³], n a dilution factor equal to the ratio of recharge from agricultural areas to total recharge, $g'(t)$ the

modified transfer function and $\lambda_{\text{pesticide}}$ the first order degradation rate of the pesticide in the aquifer [1/T].

2.6 Delineation tool

The delineation algorithm is based on a spatial optimization of the pesticide mass balance: if pesticides applied on an area of the plateau are detected in a spring, then this particular area has to be hydraulically connected to the spring. A mass balance can thus be calculated between pesticide measured in a spring and its contributing areas, and consequently constitutes useful information concerning the geometry of the spring's recharge area. In an approach similar to that of a mixing cell model (Adar, 1984), the study area H is subdivided into a discrete set of well-mixed compartments (or grid cells) denoted h , each of which defined by its pesticide leaching rate m_h [$\mu\text{g}/\text{m}^2/\text{y}$] (a positive number for arable land cells, and equal to zero for all other land use cells). All cells are then simultaneously assigned to one of the springs in the study area to achieve mass balance. The model is stationary and conservative, the pesticide composition of each cell is constant in time, and decay within each cell is not considered.

To find the optimal catchment surface for all springs simultaneously, the following linear program is solved

minimize

$$(4) D(x_{h,s}) = \sum_{h,s} d(h,s) \times x_{h,s}$$

subject to the pesticide mass balance

$$(5) q_s \times c_s \leq \sum_{h \in H} m_h \times x_{h,s}, \quad \forall s$$

$$0 \leq x_{h,s} \leq x_{\text{max}}, \quad \forall (s, h)$$

where $D(x_{h,s})$ is the total transport “cost” of the pesticide from its leaching cells to the springs, $d(h,s)$ is a cost-distance function, $x_{h,s}$ [m^2] the recharge surface in cell h connected to spring s , q_s [l/y] the annual groundwater discharge, c_s [$\mu g/l$] is the average pesticide concentration detected in spring s in cell h , m_h [$\mu g/y$] is the pesticide mass leached at steady-state during a year and x_{max} is the surface of a cell (every cell is considered to have the same surface).

The cost-distance function was considered here to describe implicitly the probability that a point is hydraulically connected to the spring, i.e. the closer a point is to the spring, the more probable is the connection between the two (see Appendix A). Two functions, the first isotropic and the other anisotropic, were used. The isotropic function is the Euclidean distance between a spring and a cell raised to a power k ($k \geq 1$),

$$(6) \quad d(h,s) = \|h-s\|_2^k,$$

and thus defines concentric isolines centered on the spring. To obviate obtaining circular catchments, the computing domain is restricted to areas situated upgradient of each spring. The anisotropic cost-distance matrix is derived from a two-dimensional random walk (see annex)

$$(7) \quad d(h,s) = (pq)^{-\|h-s\|_2} \times p^{-\sin\alpha_s} \times q^{-\cos\alpha_s}$$

where p is the probability for water to follow the direction of the groundwater gradient α_s , and q the complementary event.

The optimal solution of the optimization problem $x_{h,s}^*$ determines only the part of the recharge area that is a pesticide source (arable land).

Every compartment is a source directly connected to a spring without any kind of flow routing involved, which is not the case in a classical mixing-cell model, where most cells along a flowpath are only indirectly connected to a source through neighbouring cells. Nevertheless, it is clear from Eq. 5 that a cell h is connected to a spring s if and only if the surface of the recharge zone $x_{h,s} > 0$.

2.7 Delineation runs

The delineation tool was run for a cell resolution of 20 square meters using the atrazine soil leaching rates calculated above, increased by 10% to give some leeway to the model. The minimization problem has been written in the General Algebraic Modeling System (GAMS, Andersen and Andersen, 1999) and solved by the convex solver Mosek (Rosenthal, 1988).

Four sets of runs were performed. First, the isotropic cost-distance function was used with a simple leaching map consisting of the two leaching rates for the northern and southern region and an exponent k equal to 1. Then, the isotropic function was replaced by the anisotropic function given in Eq. 7 introducing *a priori* a main flow direction derived from a digital elevation model assuming that for the sandstone cuesta the water table is topography controlled (Haitjema and Mitchell-Bruker, 2005). Thirdly, a leaching map taking into account different application frequencies was introduced. In a fourth step, the spatial variability of the leaching rate was increased further by adding a stochastic component to the leaching map.

In run 1 and run 2, atrazine was assumed to have been applied on a regular basis on all arable land available. For run 3, a more realistic leaching map was derived from the crop rotation dataset. The frequency in years (4/4, 3/4, 2/4, 1/4 and 0) with which maize had been grown on each arable plot of the plateau between 2006 and 2009 was computed.

In order to test the effect of spatially variable leaching concentrations on the results of run 3, the leaching rate for each frequency class defined in run 3 was allowed to vary for each cell according to lognormal law which was chosen to reflect the multiplicative effect of small

random processes on pesticide leaching concentration (Ott, 1990). The spread of each log-normal distribution was set so that the highest values for a given application frequency would slightly overlap with the median of the next upper class. 300 random leaching maps were generated, yielding 300 different recharge areas. Finally, the 50% isoline of the 300 runs was calculated (Figure 5c).

3. Results

3.1 Pesticides in spring water

The herbicide atrazine was detected in all but one spring, whereas bentazone and n,n-dimethylsulfamide, a metabolite of tolylfluanide, were detected regularly in some springs only. Atrazine concentrations were stable over time, displaying neither trends nor seasonal variations. The absence of seasonal variations in the measured pesticide concentrations is a first indication that the fast flow component is small. As shown in figure 3, five distinct pollution groups are recognizable along the springs emerging on the western side of the study area (K1 to K6, K7 to K13, K14 to K18, K19 to K21, K21a), showing alternating and mutually exclusive pollution patterns of bentazone and n,n-dimethylsulfamide. Since atrazine was present in all but one spring, it was selected to run the delineation algorithm. n,n-dimethylsulfamide was used for model validation. Variations in the concentrations along the south-north profile reflect either the magnitude of atrazine leaching, the different ratios of agricultural area to total contributing surface or the application dose. The spatial variability of the latter was ignored for lack of appropriate data.

3.2 Soil residence time

Figure 4 a. shows the predicted evolution of atrazine concentration in recharge water after the last soil application for the three different soil hydraulic parameter sets. Although the absolute simulated values at steady-state differed by a factor of three between highest and lowest predictions, the ratio of biennial or triennial to annual application was comparable for

all hydraulic parameterizations ($c'_{tri}/c'_{annual} \approx 2/11$ and $c'_{bi}/c'_{annual} \approx 4/11$). These ratios are different from 1/3 and 1/2 due to non-linear sorption effects. All models also predict similar evolution in leaching after the last application. Atrazine continues to be released from the soil for about three years at a similar rate after which concentrations begin to decrease sharply. Leaching in the nanogram concentration range decreases to less than half its steady-state value after four years and drops below the limit of quantification of 5 ng/L after seven years. The onset of leaching to groundwater after the first application follows the same pattern, simply reversed in time. The inertia of the soil was implemented in the leaching scenario presented in the paragraph on soil dynamics by adding four years to the leaching period after the atrazine ban came into force in Luxembourg in 2005.

3.3 Fast flow component

Overall, discharge in the springs is characterized by its small variance (coefficient of variation below 0.1). The annual recharge cycle was clearly observed in the continuous discharge and temperature measurements, which were otherwise uncorrelated with particular rain events, even after heavy storms. Deuterium measurements varied mostly within the range of analytical error of ± 1 ‰. A few more pronounced deviations were observed, rarely lasting for more than two consecutive weeks. Hydrograph separation applied to these events showed that fast flow in spring discharge never exceeded 15% of total spring discharge, even after heavy rain events (Farlin et al., 2013). During fast flow surges lasting for more than a week, weekly measurements of spring water chemistry and pesticide concentrations did not vary significantly or systematically.

3.4 Slow flow component

Tritium concentration in the springs ranged from 7 to 10 TU and the calculated mean residence times ranged from 10 to 17 years. Such mean residence times lead to an efficient smoothing of interannual variations in the leaching. Consequently, a constant annual leaching to the groundwater was assumed for the period 1970 to 2009 and was simulated by

a step function. Atrazine concentration in spring water over time was calculated using equation 3 (figure 4). According to predictions in the aquifer, atrazine concentration had, in 2008 approximately, reached at least 90% of its maximum value (equal to 45% of the steady-state soil leaching concentration due to dilution caused by atrazine-free forest recharge). This agrees with the stable atrazine concentrations in spring water over the observation period. Degradation reduces the absolute concentrations without modifying the overall shape of the breakthrough curve (Farlin et al., 2013), as shown in figure 4 for degradation rates of 0.07, 0.03 and 0.02 1/y corresponding to a half-life of 10, 20 and 30 years respectively.

3.5 Atrazine leaching

For the delineation, the average value of pesticide leaching out of the sandy soils must be estimated with as much accuracy as possible, as the surface assigned to each spring is inversely proportional to the leaching value per surface area. Pesticide concentration measured in a spring is controlled by two factors. The proportion of cultivated surfaces in the zone of recharge constitutes the primary control, but the pesticide flux leached from each field, which depends on the soil's hydraulic and chemical properties and on the atrazine application cycles and application rates, may also vary both in time and space (Dubus et al., 2003). As the mean atrazine concentration measured in spring water is stable and near its maximum (figure 4) and all the springs draining the plateau have been sampled, the long-term average atrazine leaching can be calculated from the total mass discharged from the plateau in a year divided by the crop land area.

First, the springs were assigned to one of the two regions (north or south of the woodland strip) using the water balance. Then, the total atrazine mass discharged from each region in a year was calculated from its concentration in spring water. Finally, the surface area of atrazine leaching for each region was estimated from the crop rotation dataset, assuming only maize culture had been treated and that the crop rotation for the years 2006 to 2009 was representative of the agricultural practices on the plateau over a longer period. In order to illustrate the uncertainties in the total leaching surface, the leaching rates calculated using

both the realistic land use distribution and the total arable land surface area available are shown in *Table 1*.

Table 1 Atrazine annual leaching. The leaching rates for atrazine were calculated from the total mass discharge in the springs in one year divided by the surface area of arable land planted with maize. Values in brackets are for the total arable land surface area on the plateau

	arable land surface	atrazine mass discharged	annual atrazine
	area [ha]	in spring water [g/y]	leaching [$\mu\text{g}/\text{m}^2/\text{y}$]
North	124 (193)	13.6	10.9 (7)
South	57 (60)	2.2	3.9 (3.7)

The difference in the annual atrazine masses between both regions is striking, and cannot be accounted for solely by the uncertainty in the field surface area belonging to each region. The mean atrazine mass discharged from the northern region, two to three times higher than in the south, could be due to the sandier texture of the soils. The higher hydraulic conductivity of the sandy soils increases the speed with which pesticides are flushed out of the biologically active soil zone and reduce accordingly the degradation time in the topsoil, hence leading to higher leaching concentrations to the groundwater. The atrazine concentration measured in the monitoring well, varying seasonally from 30 to 45 ng/l, was 25 to 50% lower than the concentration obtained by dividing the annual atrazine leaching rate of the northern region by the annual recharge of 180 mm (Eq. 8). The estimated atrazine concentration in Eq. 8 is however an overestimate, since the recharge for cropland is probably higher than the 180 mm calculated for the entire plateau, which represents a mean value for all land uses.

$$(8) \quad C'_{\text{atrazine}} = \frac{m_{\text{atrazine}}}{R} = \frac{11000}{180} = 61$$

with C_{atrazine}' =atrazine concentration in groundwater [ng/l], m_{atrazine} =atrazine mass leached per square meter and year [ng/m²/y] and R =annual recharge [mm/y]

3.6 Delineation of the recharge areas

Except for the springs of the southern region (K1 to K6), the springs on the western slope were grouped according to the pollution pattern shown in figure 3. Springs K3 to K6 were also regrouped, since the discharge of each spring is much lower than in K1, K2 and K7. Figure 5 displays the recharge areas computed for runs 1 and 4 (runs 2 and 3 not shown) and Table 2 the means and standard deviations of the log-normal model used for runs 3 and 4. For runs 3 and 4, the mass balance was calculated as described in the previous

paragraph, except that each plot was weighted by the ratio $\frac{C_{\text{frequency}}'}{C_{\text{annual}}'}$ calculated by PEARL..

The resulting leaching map was then used in conjunction with the isotropic cost-distance function. For the stochastic simulations (run 4), the means were the same as for run 3 and the standard deviations were those given in Table 2.

Table 2 Leaching concentrations for the different application frequencies and standard deviations used for the Monte Carlo simulations assuming a log-normal model

Application frequency	C_{north} [$\mu\text{g}/\text{m}^2/\text{y}$]	σ_{north}	C_{south} [$\mu\text{g}/\text{m}^2/\text{y}$]	σ_{south}
1/4	5	ln(1.4)	2	ln(1.5)
2/4	14	ln(1.2)	6	ln(1.2)
3/4	25	ln(1.2)	11	ln(1.2)
4/4	39	ln(1.2)	17	ln(1.2)

The shape and spatial distribution of the spring catchments for run 1 are both intuitive and reasonable. On the contrary, delineation using the anisotropic cost-distance function (run 2) resulted in obvious artifacts. Some catchments were discontinuous, or cut off from the

springs draining them by other catchments, and the boundaries often had counterintuitive shapes (sharp corners, curvatures). For isolated springs such as the light blue northernmost spring, the shapes predicted by run 1 and 2 reflect the underlying cost-distance function: concentric for the isotropic function, and directed for the anisotropic one.

Integrating a spatially distributed leaching map based on recorded crop rotation did not increase the plausibility of model results and resulted in fragmented recharge zones partially cut off from the associated springs. For the southern fields the overall pattern was similar between run 1 and 3, since the leaching map did not differ much from the map with constant leaching values used for run 1. The northern recharge zones were however vastly different between run 1 and 3 and extremely erratic for run 3, as maize culture frequency (and consequently atrazine leaching) was much less homogeneous than in the southern part of the plateau. Similarly to run 2, most recharge zones were discontinuous, and sometimes cut off from its respective spring by other recharge zones. Additionally, the linear cost-function proved inadequate when the leaching rate is spatially distributed, because selecting cells farther away from the spring but with a higher leaching rate (for instance a leaching rate of $2 \mu\text{g}/\text{m}^2/\text{y}$ for an application frequency of $1/4 \text{ 1/y}$ versus $6 \mu\text{g}/\text{m}^2/\text{y}$ for an application frequency of $2/4 \text{ 1/y}$) can lead to a lower total transport cost. To enforce the selection of the nearest cells, the exponent k in Eq. 6 was increased in run 4 to counterbalance the effect of higher leaching-rate areas being farther away from the spring than areas with lower leaching rates. The computed recharge areas became more regular as the exponent increased and stabilized for exponent values of 8 and higher.

The delineation procedure was also applied to the springs situated on the eastern side of the Alzette valley, but provided little additional information on the spatial distribution of the recharge areas for two complementary reasons. This is due firstly to the lower density of springs draining the aquifer on this side of the valley, leading to badly defined lateral constraints, and secondly to the low atrazine concentration in all the springs, indicating that

agricultural areas make out a small portion of the recharge area only so that the information gain due to atrazine is small compared to the large degree of spatial freedom.

3.7 Model verification

Tolylfluanide, the parent compound of n,n-dimethylsulfamide, is a herbicide commonly used in commercial fruit orchards. Hence, the plausibility of the model results could be tested by comparing the recharge zones of run 1 and run 4 with the pollution pattern of n,n-dimethylsulfamide displayed in figure 3. The delineation would be consistent with observations if an orchard is enclosed in or adjacent to the recharge zones of springs polluted with the compound. The most probable source of n,n-dimethylsulfamide for the group of springs K7 to K13 is orchard 1, while the source for the pollution observed in K19 to K21 is probably orchard 3 (orchard 2 is not commercially exploited). In run 1, orchard 1 is surrounded on three sides by the recharge area of the springs K7 to K13, and although the extreme boundaries of the K19 to K21 group do not extend far enough towards orchard 3, the recharge zone is still situated directly downstream of a line running from the orchard to the springs. Additionally, the recharge area of the spring K21a, where n,n-dimethylsulfamide is below detection limit, is correctly situated farther away to the north west. The results are also consistent with the groundwater dating results: the longer the mean residence times, the more elongated the recharge area (the estimated groundwater residence times are given in Appendix B).

The results of run 4 are still qualitatively consistent with those of run 1 concerning the n,n-dimethylsulfamide patterns, but less clear. The recharge area of the springs K7 to K13 in particular is less compact than for run 1, and the recharge area of spring K21a extends much farther to the west towards orchard 3.

4. Discussion

The major strength of the model presented here is to use objectively the information conveyed by a given pesticide concerning its source within the catchment. It is also simple

enough to be implemented in a fractured rock setting, as long as fast flow is negligible and the pesticide used as tracer is supplied by slow flow with residence times sufficiently long to smooth out seasonal and inter annual variations in the soil leaching concentration.

The model's major weaknesses lie in the assumption that over a number of years, the pesticide leaching concentration was on average similar for all fields and in the underlying cost-distance function. The surface area of each recharge zone is inversely related to the soil leaching value. Given the fractured nature of the aquifer, actual recharge areas may be much more convoluted than smooth analytical solutions of the transport equation lead one to expect (Stauffer et al., 2002). Nevertheless, recharge areas fragmented or cut off by other recharge areas from the springs to which they were assigned were considered as less plausible. The simplest linear model has been shown to be superior to its more complex counterpart both in terms of the overall shapes of the recharge zones and more decisively in terms of matching the n,n-dimethylsulfamide pattern. Including field application frequencies did not increase the plausibility of model results, even after taking the leaching uncertainty into account in a Monte Carlo simulation. Using a more realistic and spatially distributed atrazine leaching lead to extremely fragmented recharge zones, reflecting the spatially heterogeneous leaching rates, which were, in some cases, separated from their assigned spring and reproduced less well the n,n-dimethylsulfamide pollution pattern.

The model cannot be expected to extract and use information that is not present in the raw data. The approach is best suited for springs that receive a significant portion of recharge water from agricultural areas, as this orients the search algorithm. The performance of the model is poor for springs where the pesticide concentration is low, since the information content is sparse and spatially non-discriminating. For isolated springs where the lateral extent of the recharge zone is not implicitly constrained by competing catchments, the anisotropic function must be used and the flow direction set a priori, increasing the number of parameters and the variance of the model. Even if the adopted random walk model is a valid approximation of the aquifer's hydraulic behaviour, the results depend largely on the

assumed flow direction. Whenever the simplest model cannot be adopted and if the main flow direction is known or can be inferred from the topography or water table measurements, the anisotropic model still provides an alternative model.

It is important to mention that the recharge zones are calculated without calibration. Leaching values obtained from the mass balance were used without any additional fitting involved. Both the homogeneous and the spatially-distributed leaching maps lead to similar results, which constitutes a sound consistency check and shows that the model can incorporate the spatial information from a spatially distributed leaching map. The long-term representativity of the latter is unknown, but a clear correlation was found between atrazine soil residues measured in a plateau-wide sampling campaign conducted in 2009 and maize culture frequency used in the present study (Farlin et al. (2012) Assessment of pesticide soil residues as a means for constraining pesticide leaching predictions. Unpublished report).

Sorption and degradation processes in the aquifer are considered negligible in the delineation algorithm. Both assumptions are strong, but reasonable, as many studies report reduced attenuation and sorption below the soil root zone (Moreau and Mouvet, 1997, Morvan et al., 2006, Pothuluri et al., 1990). If sorption had lead to a retardation of the atrazine signal relative to water, atrazine concentration would still have been increasing during the measurement period. Since degradation losses in the aquifer were neglected, the length of the recharge zones is underestimated, as atrazine mass is lost along each flowpath. The introduced bias would increase with increasing length of the recharge area, but without data concerning degradation rate, the importance of the underestimation could not be evaluated.

5. Conclusions

A simple model based on a pesticide mass balance optimization was developed to estimate the spatial extent of the recharge area of contact springs draining the Luxembourg Sandstone. Despite the limitations discussed, the approach constitutes a simple and reliable

complement to classical groundwater protection zone delineation methods in a fractured-rock setting by integrating objectively ancillary data such as pesticide spring concentration. Additional investigation is needed to assess the importance of pesticide degradation in the aquifer as a function of transit time on the calculation of the recharge zones. Comparison between the approach presented and the results of a classical numerical groundwater model could also prove highly informative.

Acknowledgements

The authors gratefully acknowledge the funding of this work by the Luxembourg Research Fund (FNR, project SECAL/07/05). Partial support for the groundwater dating part was provided by the GENESIS project (EU no. 226536, FP7-ENV-2008-1).

References

- Adar EM (1984) Quantification of aquifer recharge distribution using environmental isotopes and regional hydrochemistry. Doctoral thesis, Univ of Arizona, Tucson, United States: 269
- Allen R, Walker A (1987) The influence of soil properties on the rates of degradation of metamitron. *Pesticide Science* 18: 95-111
- Allen RG, Pereira LS, Raes D and M Smith (1998) Crop evapotranspiration-Guidelines for computing crop water requirements. *FAO irrigation and drainage paper* 56
- Andersen, D, and KD Andersen. 1999. The MOSEK interior point optimization for linear programming: an implementation of the homogeneous algorithm. *in: Frenk JBG, Roos C, Terlaky T and Zahng S (eds) High Performance Optimization Techniques, Proceedings of the HPOPT-II conference: 197-232.*
- Benbrahim M (2004) Caractérisation hydrochimique détaillée des eaux souterraines du Luxembourg-Rapport final (Detailed hydrochemical characterisation of the groundwater in Luxembourg-final report), Luxembourgish National Research Fund: 137 pages

- Bodin J, Delay F, de Marsily G (2003) Solute transport in a single fracture with negligible matrix permeability: 1. Fundamental mechanisms. 2. Mathematical formalism. *Hydrogeology Journal* 11: 418-433, 434, 454
- Cacas MC, Ledoux E, de Marsily G, Barbreau A, Calmels P, Gaillard B, Magritta R (1990) Modeling fracture flow with a stochastic discrete fracture network: calibration and validation. 1, The transport model. *Water Resour Res* 26: 479-489
- Clark I, Fritz P (1997) *Environmental isotopes in hydrogeology*. Lewis Publishers
- Colbach R (2005) Overview of the geology of the Luxembourg Sandstone(s). *Ferrantia* 44: 155-160
- Doherty J (2009) *PEST: model-independent parameter estimation user manual*. Watermark, Brisbane, Australia
- Dubus IG, Brown C, Beulke S (2003) Sources of uncertainty in pesticide fate modeling. *Science of the Total Environment* 317: 53-72
- Eckhardt DAV, Wagenet RJ (1996) Estimation of the potential for atrazine transport in a silt loam soil. *Herbicide Metabolites in surface Water and Groundwater*, ACS Symposium Series 630 American Chemical Society, Washington, DC
- Eichinger L, Forster M, Rast H, Rauert W, Wolf M (1980) Experience gathered in low-level measurements of tritium in water. IAEA: Vienna: 43-64
- Epstein S, Mayeda TK (1953) Variations of ^{18}O content of waters from natural sources. *Geochimica Cosmochimica Acta* 4: 213-224
- Farlin J, Gallé T, Bayerle M, Pittois D, Braun C, El Khabbaz H, Maloszewski P, Elsner M (2013) Predicting pesticide attenuation in a fractured aquifer using lumped-parameter models. *Groundwater* **in print doi: 10-1111/j.1745-6584.2012.00964.x**
- FOCUS (2000) *FOCUS groundwater scenarios in the EU review of active substances*. Report of the work of the Groundwater scenarios working group of FOCUS, version 1 of 1 November 2000. EC Document Reference Sanco/321/2000 rev2: 202

- Gourdol L, Zimmer G, Pundel N, Hoffmann L, Pfister L (2010) Les sources de la ville de Luxembourg: une ressource en eau potable à préserver. 1. Aspects quantitatifs et physico-chimiques (The springs of the city of Luxembourg: a drinking water resource to protect. 1. Quantitative and physico-chemical aspects). Arch Sci Nat Phys Math NS: 101-124
- Haitjema HM, Mitchell-Bruker S (2005) Are water tables a subdued replica of the topography? Ground Water 43: 781-786
- Jura WA, Gruber J (1989) A stochastic analysis of the influence of soil and climatic variability on the estimate of pesticide groundwater potential. Water Resour Res 25: 2465-2474
- Käss W (1998) Tracing Techniques in Geohydrology. Balkema, Rotterdam: 581
- Leistra M, van der Linden AMA, Boesten JJTI, Tiktak A, van den Berg F (2001) PEARL model for pesticide behaviour and emissions in soil-plant systems. Descriptions of the processes in FOCUS PEARL v 1.1.1. Alterra-Rapport 013 RIVM report 711401009
- Lucius M (1943) Das Einzugsgebiet der Quellen der interkommunalen Wasserleitung Süd (The subsurface catchment of the springs of the intercommunal water main South). Luxembourg geological survey: 20 pages
- Maloszewski P, Benischke R, Harum T, Zojer H (1998) Estimation of solute transport parameters in a karstic aquifer using artificial tracer experiments. In: Shallow Groundwater Systems, Dillon P, Simmers I (ed), Balkema, Rotterdam: 177-190
- Maloszewski P, Willibald S, Zuber A, Rank D (2002) Identifying the flow systems in a karstic-fissured-porous aquifer, the Schneealpe, Austria, by modeling of environmental ^{18}O and ^3H isotopes. Journal of Hydrology 256: 48-59
- Marion W, Urban K (1995) TMY2s. National Solar Radiation Data Base
- Moreau C, Mouvet C (1997) Sorption and desorption of atrazine, deethylatrazine, and hydroxyatrazine by soil and aquifer solids. Journal of Environmental Quality 26: 416-424

- Morvan X, Mouvet C, Baran N, Gutierrez A (2006) Pesticides in the groundwater of a spring draining a sandy aquifer: Temporal variability of concentrations and fluxes. *Journal of Contaminant Hydrology* 87: 176-190
- Ott W (1990) A physical explanation of the Lognormality of Pollutant Concentrations. *J Air Waste Manage Assoc* 40: 1378-1383
- Pfister L, Wagner C, Vansuypeene E, Drogue G, Hoffmann L (2005) Atlas climatique du Grand-Duché de Luxembourg (climate atlas of the Grand-Duchy of Luxembourg). National museum of natural history , Public research centre Gabriel Lippmann, Administration for agriculture: 80 pages
- Pochon A, Zwahlen F (2003) Auscheidung von Grundwasserschutz zonen bei Kluffgrundwasserleitern-Praxishilfe (Delineation of ground water protection zones in fractured-rock aquifers-Practical guide). Vollzug Umwelt Bundesamt für Umwelt, Wald und Landschaft , Federal Agency for water and geology, Bern: 83 pages
- Pothuluri JV, Moorman TB, Obenhuber DC, Wauchope RD (1990) Aerobic and anaerobic degradation of alachlor in samples from a surface-to-groundwater profile. *Journal of Environmental Quality* 19: 525-530
- Rosenthal, RE 1988. GAMS: A User's Guide. *The Scientific Press, Redwood City, California.*
- Ryan M, Meiman J (1996) Change in discharge and water quality of Big Spring in response to a precipitation event. *Groundwater* 34: 23-30
- Scheidegger AE (1957) *The physics of flow through porous media.* Toronto Press
- Stauffer F, Attinger S, Zimmermann S, Kinzelbach W (2002) Uncertainty estimation of well catchments in heterogeneous aquifers. *Water Resour Res* 38: 1238-1247
- USEPA (1991) Delineation of wellhead protection areas in fractured rocks. Wisconsin Geological and Natural History Survey, Ground-Water Protection Division, Office of Groundwater and Drinking Water, US Environmental Protection Agency, Washington, DC 20460

van Dam JC, Huygen J, Wesseling JG, Feddes RA, Kabat P, van Valsum PEV, Groenendijk P, Diepen CA (1997) Theory of SWAP version 2.0. Technical Document 45, DLO Winand Staring Centre, Wageningen

Wilks DS, Wilby RL (1999) The weather generation game: a review of stochastic weather models. *Progress in Physical Geography* 3: 329-357

Zuber A, Motyka J (1994) Matrix porosity as the most important parameter of fissured rocks for solute transport at large scales. *Journal of Hydrology* 158: 19-46

Appendix A. Cost-distance matrix

As infinitely many possible cost-distance functions can be imagined, a cost-distance function based on physical consideration was derived from a random walk model. Additionally to regional faults, the Luxembourg Sandstone is fractured along two main directions approximately orthogonal to each other (NE-SW and NW-SE (Colbach, 2005)). As a first approximation, these two directions are assumed to be the only hydraulically significant ones and the hydraulic conductivity to be an anisotropic property of the aquifer that can be described by a first-order tensor spanning an ellipsoid in the two-dimensional plane (Scheidegger, 1957). Two related hydraulic properties are relevant for the problem:

- The hydraulic conductivity describing the ability of the rock medium as a whole to transmit water
- The connectivity of the fracture network

It is postulated that the probability for two given points in the two-dimensional space to be connected decreases with distance and with deviation from the major semi-axis of the anisotropy ellipsoid. Let $x(r, \theta)$ be any point in the plane with position expressed in polar coordinates (r = distance from the spring and θ = angle from the major semi-axis), and $P(x)$ the probability that x is connected to the spring, so that

$$(9) \quad P(x) \sim \frac{1}{r}$$

$$(10) \quad P(x) \sim \frac{1}{\theta}$$

Now consider a two-dimensional random walk on a square grid oriented along the major and minor axis of anisotropy and a Manhattan metrics, so that only steps parallel to one of these axes are allowed. The step size is constant, and the random walk is directed towards the spring, so that at each point, there are only two possible choices, either “down” parallel to the major semi-axis (the ordinate) or “right” parallel to the minor semi-axis (the abscissa) and towards the major semi-axis. The probability for a molecule to flow into one of these two directions is

$$(11) \quad P(s = \delta d) = p$$

and

$$(12) \quad P(s = \delta r) = 1 - p = q$$

where s is the step size and δd and δr are the respective directions (“down” and “right”).

p and q can be equal, in which case the aquifer is isotropic. Any path taken by a water molecule during its random walk to the spring can be decomposed into its two components along each axis. In Cartesian coordinates, the probability for any $x(i, j)$ to be hydraulically connected to the spring is

$$(13) \quad P(x) = q^i p^j$$

Changing to a cylindrical coordinate system by setting $i = r \cos \theta$ and $j = r \sin \theta$ yields

$$(14) \quad P(x) = p q^r \times p^{\sin \theta} \times q^{\cos \theta}$$

The cost-distance function implicitly describes the probability that a point is hydraulically connected to the spring, thus the higher the probability, the lower the cost. The cost-distance function is defined thus

$$(15) \quad d(g,s) = P(x)^{-1} = (pq)^{-r} \times p^{-\sin\theta} \times q^{-\cos\theta}$$

Groundwater flows parallel to the hydraulic gradient in isotropic media only. In two dimensions, anisotropy causes a deviation of flow direction towards the semi-major axis of the anisotropy ellipse.

Let i_1 and j_1 be the components of the hydraulic gradient along the major and minor semi-axes, i_2 the component of groundwater flow along the major semi-axis, θ_1 the angle between the hydraulic gradient and the major semi-axis, and θ_2 the angle between the groundwater flow direction and the major semi-axis and s the anisotropy factor.

$$(16) \quad i_1 = j_1 = \frac{1}{s} i_2$$

$$(17) \quad \tan(\theta_1) = \left(\frac{j_1}{i_1} \right) = 1$$

$$(18) \quad \tan(\theta_2) = \left(\frac{j_1}{i_2} \right) = \frac{1}{s} \left(\frac{j_1}{i_1} \right)$$

$$(19) \quad \tan^{-1}[\tan(\theta_2)] = \tan^{-1} \left[\frac{1}{s} \left(\frac{j_1}{i_1} \right) \right] = \tan^{-1} \left[\frac{1}{s} \right]$$

$$\Rightarrow \theta_2 = \tan^{-1} \left[\frac{1}{s} \right]$$

Thus deviation from the steepest slope can be computed for different anisotropy factors s .

This factor is related to the random walk probabilities introduced above by the relation

$$(20) \quad s = \frac{p}{q}$$

The correspondence between s and p is given in Table 3.

Table 3 Deviation of groundwater flow from the hydraulic gradient for different anisotropy factors s . p is the probability for water to flow towards the spring defined in equation 11.

s	p	Deviation [°]
1.1	0.53	3
1.2	0.55	5
1.3	0.57	7
1.4	0.58	9
1.5	0.6	11
1.6	0.62	13
1.7	0.63	15

Anisotropy was estimated from measurements of fracture orientation on outcrops around the plateau by setting s equal to the ratio of the frequency of the two dominant directions. This approach yields $s=1.7$, so the maximum deviation of the groundwater flow from the hydraulic gradient was assumed to be about 15 degrees and p was set equal to 0.63 in Eq. 7.

Appendix B. Groundwater residence times

Table 4. Estimated groundwater residence times

spring	mean residence time [years]
K 1	14
K 2	14
K 3	10
K 4	12
K 5	11
K 6	13
K 7	12
K 7a	13
K 8	13
K 9	14
K 11	12
K 13	12
K 14	12
K 16	14
K 17	14
K 18	15
K 19	13
K 20	14
K 21	16
K 21a	16

FIGURE CAPTIONS:

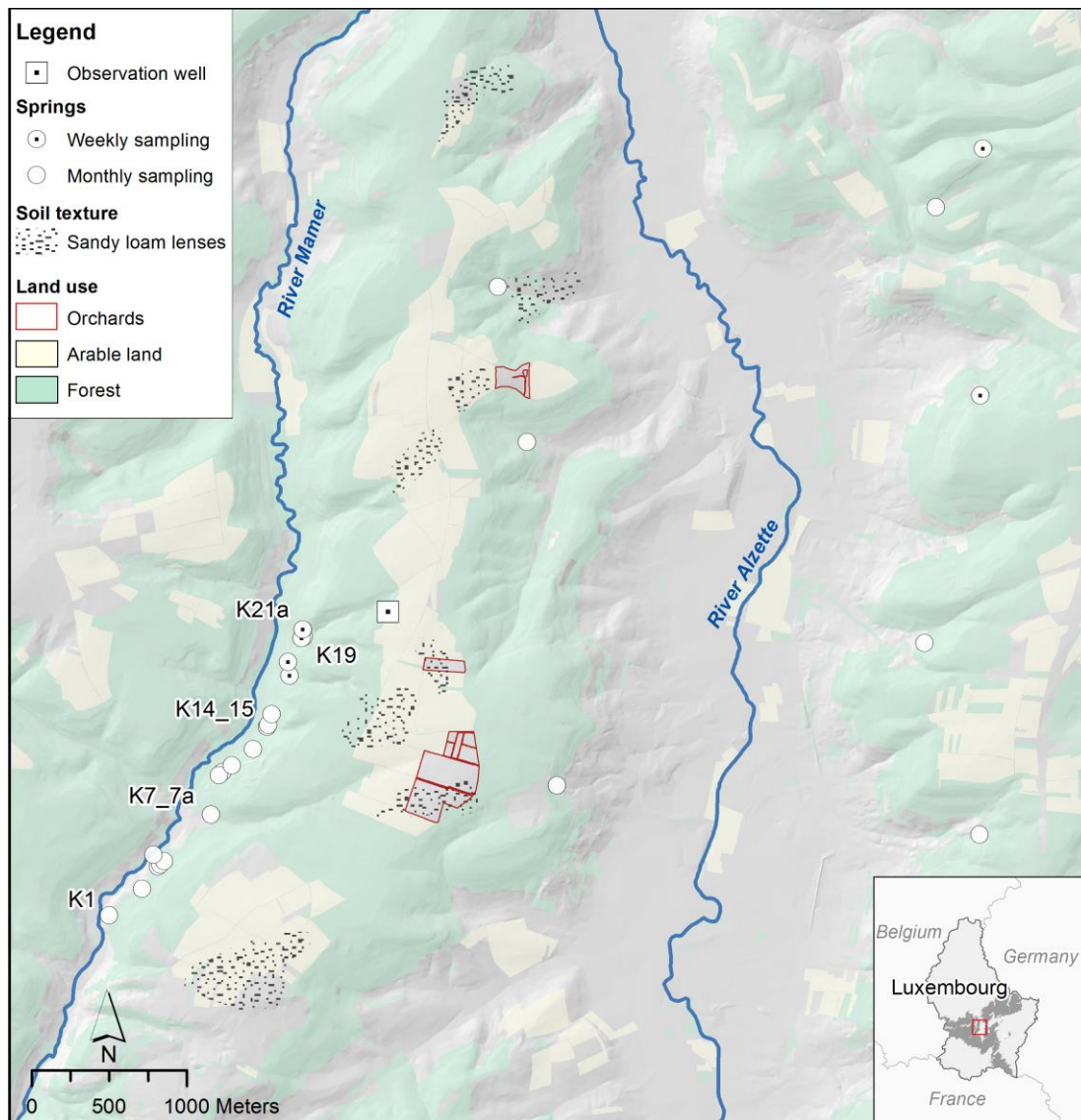


Fig 1 Study area. The Steinsel plateau, oriented north-south, is divided into two main agricultural areas by a forested strip of land. Except where indicated otherwise, the main soil type on the plateau is loamy sand. The extent of the Luxembourg Sandstone is shown in grey in the inset map

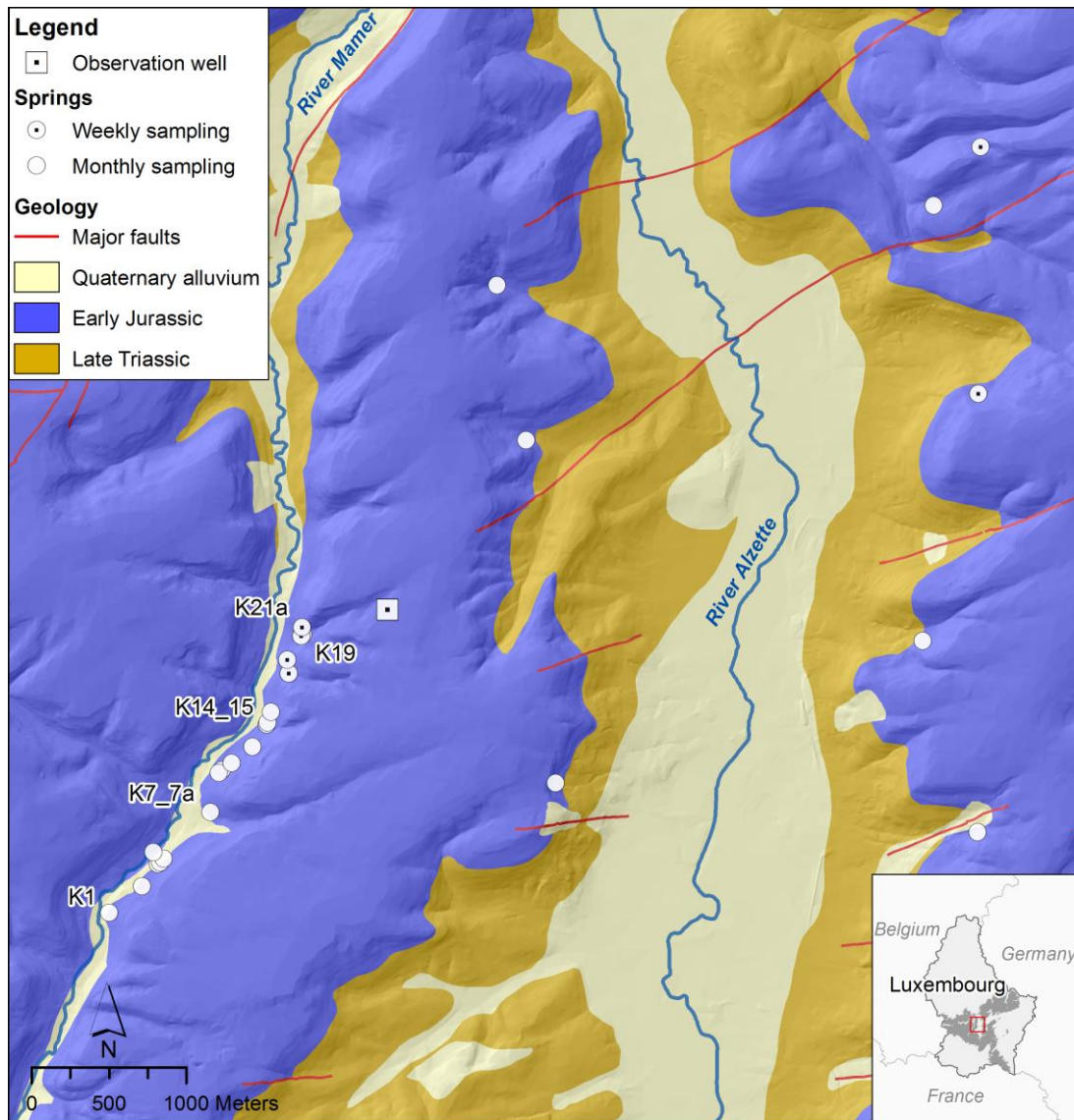


Fig 2 Geology of the study area. The main units of the Early Jurassic are: Luxembourg Sandstone, marls of Elvange; for the Late Triassic: Rhaetian clay, Carnian and Norian sandstones. The extent of the Luxembourg Sandstone is shown in grey in the inset map

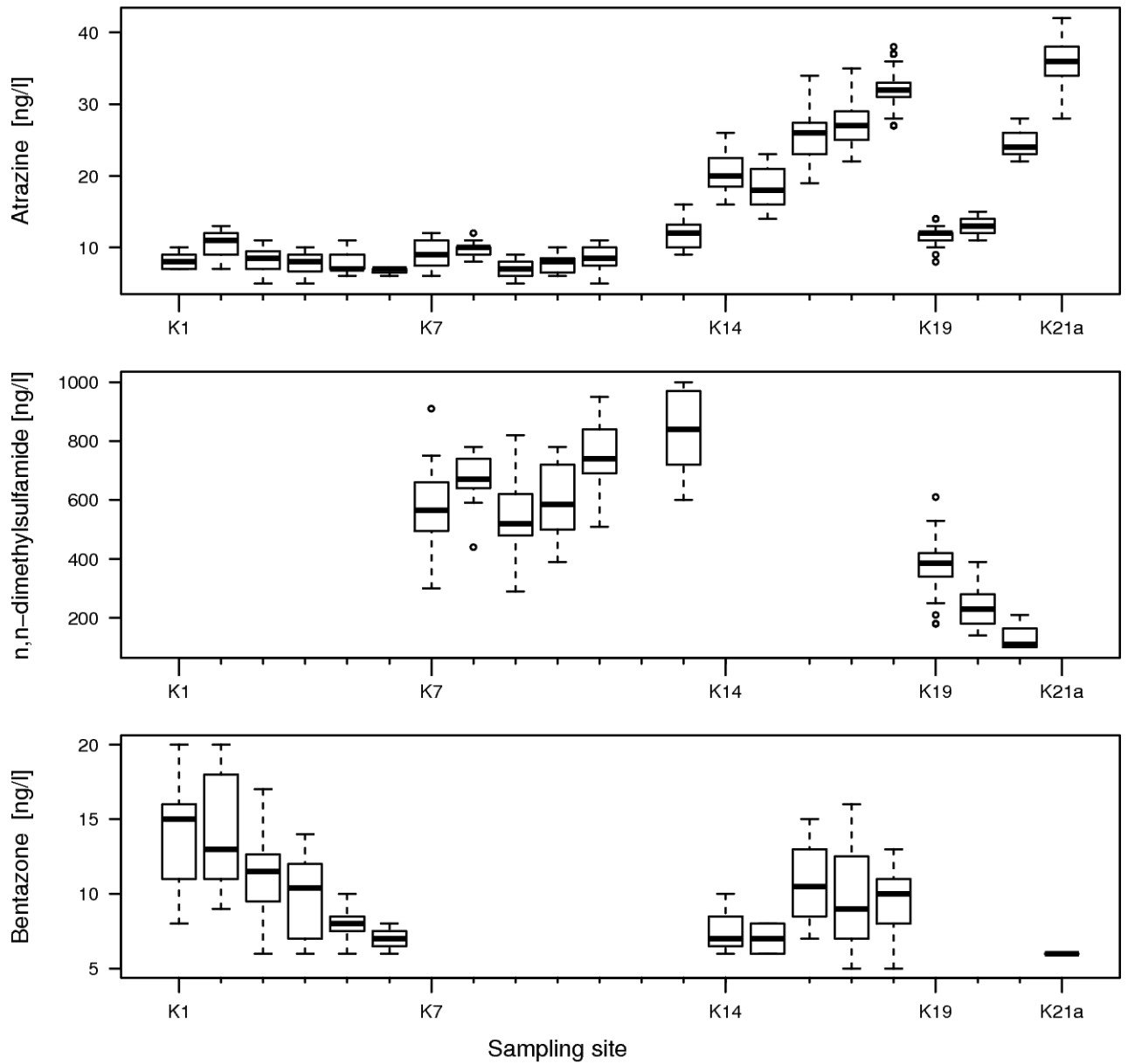


Fig 3 Pollution patterns of the springs emerging on the western side of the Steinsel plateau from south (K1) to north (K21a). Atrazine was present in concentrations above detection limit in all but one spring. Bentazone and n,n-dimethylsulfamide were never detected together in the same spring and define an alternating pattern of five spring pollution groups

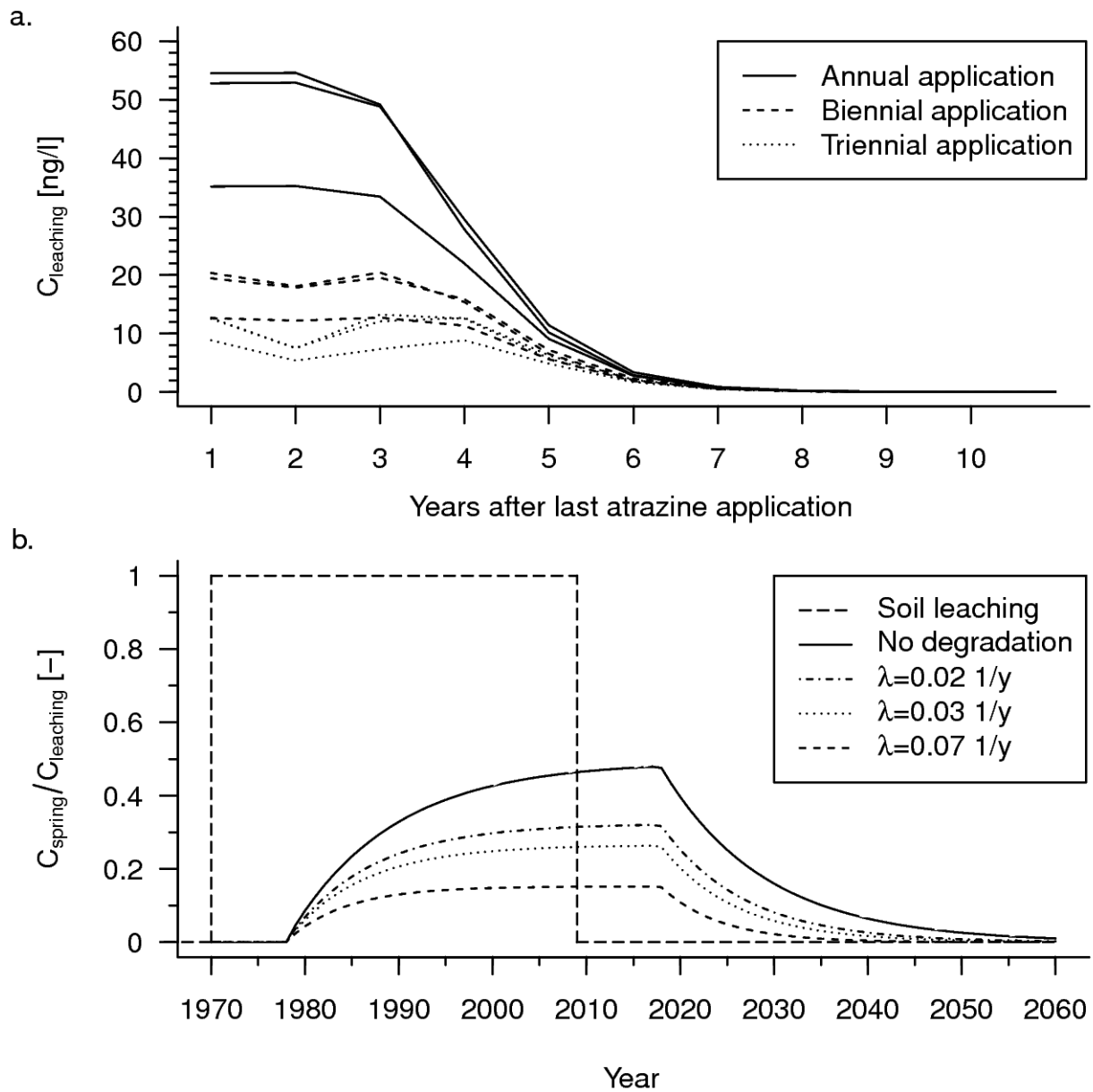


Fig 4 Atrazine dynamics in the soil and aquifer. a. Atrazine concentration over time in recharge water after the last soil application for three different soil hydraulic parameterization and application frequencies. b. Atrazine input function and spring response normalized by the steady-state soil leaching concentration for a dilution factor $n=2$ and different degradation rates $\lambda_{\text{atrazine}}$ [1/y]

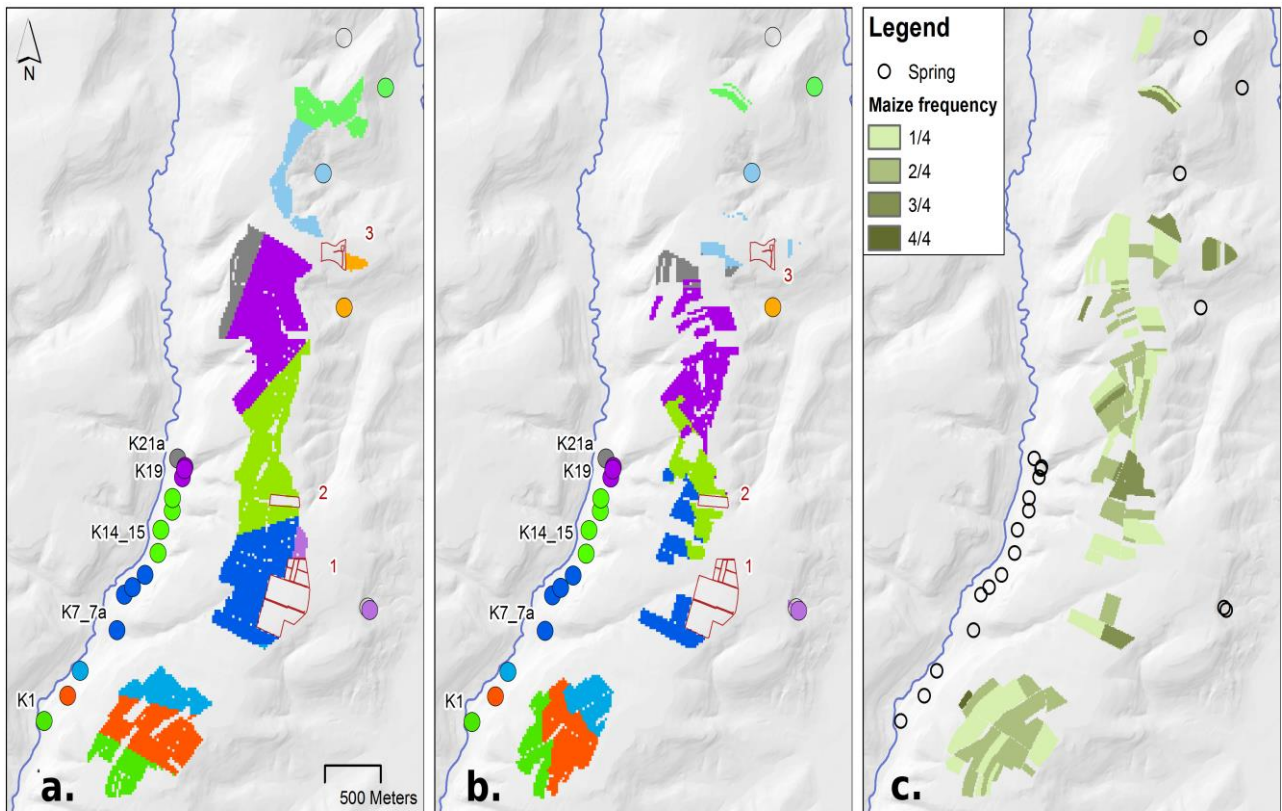


Fig 5 Comparison of the results of runs 1 and 4 (a and b) and maize culture frequency (c). a: isotropic simulation, b: Monte Carlo simulations; the three commercial orchards are numbered in red from 1 to 3. A spring or group of springs and its corresponding catchment are shown in the same colour. Labeled springs are identical to those shown on figure 2. The leaching map derived from the frequency of maize culture (c) was used to calculate the recharge areas of runs 3 and 4. For the stochastic simulations of run 4, recharge zones selected on more than 50% of the 300 runs are shown

NOTE DI LAVORO DELLA FONDAZIONE ENI ENRICO MATTEI

Fondazione Eni Enrico Mattei Working Paper Series

Our Note di Lavoro are available on the Internet at the following addresses:

<http://www.feem.it/getpage.aspx?id=73&sez=Publications&padre=20&tab=1>
http://papers.ssrn.com/sol3/JELJOUR_Results.cfm?form_name=journalbrowse&journal_id=266659
<http://ideas.repec.org/s/fem/femwpa.html>
<http://www.econis.eu/LNG=EN/FAM?PPN=505954494>
<http://ageconsearch.umn.edu/handle/35978>
<http://www.bepress.com/feem/>

NOTE DI LAVORO PUBLISHED IN 2014

CCSD	1.2014	Erin Baker, Valentina Bosetti, Karen E. Jenni and Elena Claire Ricci: Facing the Experts: Survey Mode and Expert Elicitation
ERM	2.2014	Simone Tagliapietra: Turkey as a Regional Natural Gas Hub: Myth or Reality? An Analysis of the Regional Gas Market Outlook, beyond the Mainstream Rhetoric
ERM	3.2014	Eva Schmid and Brigitte Knopf: Quantifying the Long-Term Economic Benefits of European Electricity System Integration
CCSD	4.2014	Gabriele Standardi, Francesco Bosello and Fabio Eboli: A Sub-national CGE Model for Italy
CCSD	5.2014	Kai Lessmann, Ulrike Kornek, Valentina Bosetti, Rob Dellink, Johannes Emmerling, Johan Eyckmans, Miyuki Nagashima, Hans-Peter Weikard and Zili Yang: The Stability and Effectiveness of Climate Coalitions: A Comparative Analysis of Multiple Integrated Assessment Models
CCSD	6.2014	Sergio Currarini, Carmen Marchiori and Alessandro Tavoni: Network Economics and the Environment: Insights and Perspectives
CCSD	7.2014	Matthew Ranson and Robert N. Stavins: Linkage of Greenhouse Gas Emissions Trading Systems: Learning from Experience
CCSD	8.2013	Efthymia Kyriakopoulou and Anastasios Xepapadeas: Spatial Policies and Land Use Patterns: Optimal and Market Allocations
CCSD	9.2013	Can Wang, Jie Lin, Wenjia Cai and ZhongXiang Zhang: Policies and Practices of Low Carbon City Development in China
ES	10.2014	Nicola Genovese and Maria Grazia La Spada: Trust as a Key Variable of Sustainable Development and Public Happiness: A Historical and Theoretical Example Regarding the Creation of Money
ERM	11.2014	Ujjayant Chakravorty, Martino Pelli and Beyza Ural Marchand: Does the Quality of Electricity Matter? Evidence from Rural India
ES	12.2014	Roberto Antonietti: From Outsourcing to Productivity, Passing Through Training: Microeconomic Evidence from Italy
CCSD	13.2014	Jussi Lintunen and Jussi Uusivuori: On The Economics of Forest Carbon: Renewable and Carbon Neutral But Not Emission Free
CCSD	14.2014	Brigitte Knopf, Bjørn Bakken, Samuel Carrara, Amit Kanudia, Ilkka Keppo, Tiina Koljonen, Silvana Mima, Eva Schmid and Detlef van Vuuren: Transforming the European Energy System: Member States' Prospects Within the EU Framework
CCSD	15.2014	Brigitte Knopf, Yen-Heng Henry Chen, Enrica De Cian, Hannah Förster, Amit Kanudia, Ioanna Karkatsouli, Ilkka Keppo, Tiina Koljonen, Katja Schumacher and Detlef van Vuuren: Beyond 2020 - Strategies and Costs for Transforming the European Energy System
CCSD	16.2014	Anna Alberini, Markus Bareit and Massimo Filippini: Does the Swiss Car Market Reward Fuel Efficient Cars? Evidence from Hedonic Pricing Regressions, a Regression Discontinuity Design, and Matching
ES	17.2014	Cristina Bernini and Maria Francesca Cracolici: Is Participation in Tourism Market an Opportunity for Everyone? Some Evidence from Italy
ERM	18.2014	Wei Jin and ZhongXiang Zhang: Explaining the Slow Pace of Energy Technological Innovation: Why Market Conditions Matter?
CCSD	19.2014	Salvador Barrios and J. Nicolás Ibañez: Time is of the Essence: Adaptation of Tourism Demand to Climate Change in Europe
CCSD	20.2014	Salvador Barrios and J. Nicolás Ibañez Rivas: Climate Amenities and Adaptation to Climate Change: A Hedonic-Travel Cost Approach for Europe
ERM	21.2014	Andrea Bastianin, Marzio Galeotti and Matteo Manera: Forecasting the Oil-gasoline Price Relationship: Should We Care about the Rockets and the Feathers?
ES	22.2014	Marco Di Cintio and Emanuele Grassi: Wage Incentive Profiles in Dual Labor Markets
CCSD	23.2014	Luca Di Corato and Sebastian Hess: Farmland Investments in Africa: What's the Deal?
CCSD	24.2014	Olivier Beaumais, Anne Briand, Katrin Millock and Céline Nauges: What are Households Willing to Pay for Better Tap Water Quality? A Cross-Country Valuation Study
CCSD	25.2014	Gabriele Standardi, Federico Perali and Luca Pieroni: World Tariff Liberalization in Agriculture: An Assessment Following a Global CGE Trade Model for EU15 Regions
ERM	26.2014	Marie-Laure Nauleau: Free-Riding on Tax Credits for Home Insulation in France: an Econometric Assessment Using Panel Data

CCSD	27.2014	Hannah Förster, Katja Schumacher, Enrica De Cian, Michael Hübler, Ilkka Keppo, Silvana Mima and Ronald D. Sands: European Energy Efficiency and Decarbonization Strategies Beyond 2030 – A Sectoral Multi-model Decomposition
CCSD	28.2014	Katherine Calvin, Shonali Pachauri, Enrica De Cian and Ioanna Mouratiadou: The Effect of African Growth on Future Global Energy, Emissions, and Regional Development
CCSD	29.2014	Aleh Cherp, Jessica Jewell, Vadim Vinichenko, Nico Bauer and Enrica De Cian: Global Energy Security under Different Climate Policies, GDP Growth Rates and Fossil Resource Availabilities
CCSD	30.2014	Enrica De Cian, Ilkka Keppo, Johannes Bollen, Samuel Carrara, Hannah Förster, Michael Hübler, Amit Kanudia, Sergey Paltsev, Ronald Sands and Katja Schumacher: European-Led Climate Policy Versus Global Mitigation Action. Implications on Trade, Technology, and Energy
ERM	31.2014	Simone Tagliapietra: Iran after the (Potential) Nuclear Deal: What's Next for the Country's Natural Gas Market?
CCSD	32.2014	Mads Greker, Michael Hoel and Knut Einar Rosendahl: Does a Renewable Fuel Standard for Biofuels Reduce Climate Costs?
CCSD	33.2014	Edilio Valentini and Paolo Vitale: Optimal Climate Policy for a Pessimistic Social Planner
ES	34.2014	Cristina Cattaneo: Which Factors Explain the Rising Ethnic Heterogeneity in Italy? An Empirical Analysis at Province Level
CCSD	35.2014	Yasunori Ouchida and Daisaku Goto: Environmental Research Joint Ventures and Time-Consistent Emission Tax
CCSD	36.2014	Jaime de Melo and Mariana Vijil: Barriers to Trade in Environmental Goods and Environmental Services: How Important Are They? How Much Progress at Reducing Them?
CCSD	37.2014	Ryo Horii and Masako Ikefuji: Environment and Growth
CCSD	38.2014	Francesco Bosello, Lorenza Campagnolo, Fabio Eboli and Ramiro Parrado: Energy from Waste: Generation Potential and Mitigation Opportunity
ERM	39.2014	Lion Hirth, Falko Ueckerdt and Ottmar Edenhofer: Why Wind Is Not Coal: On the Economics of Electricity
CCSD	40.2014	Weij Jin and ZhongXiang Zhang: On the Mechanism of International Technology Diffusion for Energy Productivity Growth
CCSD	41.2014	Abeer El-Sayed and Santiago J. Rubio: Sharing R&D Investments in Cleaner Technologies to Mitigate Climate Change
CCSD	42.2014	Davide Antonioli, Simone Borghesi and Massimiliano Mazzanti: Are Regional Systems Greening the Economy? the Role of Environmental Innovations and Agglomeration Forces
ERM	43.2014	Donatella Baiardi, Matteo Manera and Mario Menegatti: The Effects of Environmental Risk on Consumption: an Empirical Analysis on the Mediterranean Countries
CCSD	44.2014	Elena Claire Ricci, Valentina Bosetti, Erin Baker and Karen E. Jenni: From Expert Elicitations to Integrated Assessment: Future Prospects of Carbon Capture Technologies
CCSD	45.2014	Kenan Huremovic: Rent Seeking and Power Hierarchies: A Noncooperative Model of Network Formation with Antagonistic Links
CCSD	46.2014	Matthew O. Jackson and Stephen Nei: Networks of Military Alliances, Wars, and International Trade
CCSD	47.2014	Péter Csóka and P. Jean-Jacques Herings: Risk Allocation under Liquidity Constraints
CCSD	48.2014	Ahmet Alkan and Alparslan Tuncay: Pairing Games and Markets
CCSD	49.2014	Sanjeev Goyal, Stephanie Rosenkranz, Utz Weitzel and Vincent Buskens: Individual Search and Social Networks
CCSD	50.2014	Manuel Förster, Ana Mauleon and Vincent J. Vannetelbosch: Trust and Manipulation in Social Networks
CCSD	51.2014	Berno Buechel, Tim Hellmann and Stefan Köllner: Opinion Dynamics and Wisdom under Conformity
CCSD	52.2014	Sofia Priazhkina and Frank Page: Formation of Bargaining Networks Via Link Sharing
ES	53.2014	Thomas Longden and Greg Kannard: Rugby League in Australia between 2001 and 2012: an Analysis of Home Advantage and Salary Cap Violations
ES	54.2014	Cristina Cattaneo, Carlo V. Fiorio and Giovanni Peri: What Happens to the Careers of European Workers when Immigrants "Take their Jobs"?
CCSD	55.2014	Francesca Sanna-Randaccio, Roberta Sestini and Ornella Tarola: Unilateral Climate Policy and Foreign Direct Investment with Firm and Country Heterogeneity
ES	56.2014	Cristina Cattaneo, Carlo V. Fiorio and Giovanni Peri: Immigration and Careers of European Workers: Effects and the Role of Policies
CCSD	57.2014	Carlos Dionisio Pérez Blanco and Carlos Mario Gómez Gómez: Drought Management Plans and Water Availability in Agriculture. A Risk Assessment Model for a Southern European Basin
CCSD	58.2014	Baptiste Perrissin Fabert, Etienne Espagne, Antonin Pottier and Patrice Dumas: The Comparative Impact of Integrated Assessment Models' Structures on Optimal Mitigation Policies
CCSD	59.2014	Stuart McDonald and Joanna Poyago-Theotoky: Green Technology and Optimal Emissions Taxation
CCSD	60.2014	ZhongXiang Zhang: Programs, Prices and Policies Towards Energy Conservation and Environmental Quality in China
CCSD	61.2014	Carlo Drago, Livia Amidani Aliberti and Davide Carbonai: Measuring Gender Differences in Information Sharing Using Network Analysis: the Case of the Austrian Interlocking Directorship Network in 2009
CCSD	62.2014	Carlos Dionisio Pérez Blanco and Carlos Mario Gómez Gómez: An Integrated Risk Assessment Model for the Implementation of Drought Insurance Markets in Spain
CCSD	63.2014	Y. Hossein Farzin and Ronald Wendner: The Time Path of the Saving Rate: Hyperbolic Discounting and Short-Term Planning
CCSD	64.2014	Francesco Bosello and Ramiro Parrado: Climate Change Impacts and Market Driven Adaptation: the Costs of Inaction Including Market Rigidities
CCSD	65.2014	Luca Di Corato, Cesare Dosi and Michele Moretto: Bidding for Conservation Contracts

CCSD	66.2014	Achim Voß and Jörg Lingers: What's the Damage? Environmental Regulation with Policy-Motivated Bureaucrats
CCSD	67.2014	Carolyn Fischer, Richard G. Newell and Louis Preonas: Environmental and Technology Policy Options in the Electricity Sector: Interactions and Outcomes
CCSD	68.2014	Carlos M. Gómez, C. Dionisio Pérez-Blanco and Ramon J. Batalla: The Flushing Flow Cost: A Prohibitive River Restoration Alternative? The Case of the Lower Ebro River
ES	69.2014	Roberta Distante, Ivan Petrella and Emiliano Santoro: Size, Age and the Growth of Firms: New Evidence from Quantile Regressions
CCSD	70.2014	Jaime de Melo and Mariana Vijil: The Critical Mass Approach to Achieve a Deal on Green Goods and Services: What is on the Table? How Much to Expect?
ERM	71.2014	Gauthier de Maere d'Aertrycke, Olivier Durand-Lasserve and Marco Schudel: Integration of Power Generation Capacity Expansion in an Applied General Equilibrium Model
ERM	72.2014	ZhongXiang Zhang: Energy Prices, Subsidies and Resource Tax Reform in China
CCSD	73.2014	James A. Lennox and Jan Witajewski: Directed Technical Change With Capital-Embodied Technologies: Implications For Climate Policy
CCSD	74.2014	Thomas Longden: Going Forward by Looking Backwards on the Environmental Kuznets Curve: an Analysis of CFCs, CO2 and the Montreal and Kyoto Protocols
ERM	75.2014	Simone Tagliapietra: The EU-Turkey Energy Relations After the 2014 Ukraine Crisis. Enhancing The Partnership in a Rapidly Changing Environment
CCSD	76.2014	J. Farlin, L. Drouet, T. Gallé, D. Pittois, M. Bayerle, C. Braun, P. Maloszewski, J. Vanderborght, M. Elsner and A. Kies: Delineating Spring Recharge Areas in a Fractured Sandstone Aquifer (Luxembourg) Based on Pesticide Mass Balance